Contrast reversal of the charge density wave STM image in purple potassium molybdenum bronze $K_{0.9}Mo_6O_{17}$

P. Mallet, K. M. Zimmermann, Ph. Chevalier, J. Marcus, and J. Y. Veuillen

Laboratoire d'Etudes des Propriétés Electroniques des Solides, CNRS, Boîte Postale 166, 38042 Grenoble Cedex 9, France

J. M. Gomez Rodriguez

Departamento de Fisica de la Materia Condensada C-III, 28049 Madrid, Spain

We report on a scanning tunneling microscopy (STM) investigation of the charge density wave (CDW) state of a layered oxide compound, the purple bronze $K_{0.9}Mo_6O_{17}$. The experiments have been carried out in an ultra-high-vacuum variable-temperature STM. At low temperature, we have observed a (2×2) superstructure due to the CDW state, superimposed on the atomic lattice. Spectroscopic measurements reveal a strong decrease of the density of states near the Fermi energy, consistent with the suppression of a sizable fraction of the Fermi surface below the CDW transition temperature. Finally, by simultaneous imaging at negative and positive biases, we show a complete spatial separation between occupied and empty states involved in the CDW modulation, resulting in a contrast reversal of the CDW images. [S0163-1829(99)03127-6]

INTRODUCTION

Low-temperature scanning tunneling microscopy has been used for a long time to investigate surfaces of layered systems, where electronic instabilities are often found. A unique feature of this technique is the possibility to measure the surface local density of states (LDOS) of the sample with both an atomic spatial resolution and a good energy resolution. It is very interesting for systems showing Peierls transition, since the scanning-tunneling microscopy (STM) provides direct visualization of the charge density wave (CDW) below the Peierls temperature T_p. Images of CDW have been successfully obtained since the pioneering work by Coleman *et al.* 15 years ago, mostly for transition-metal chalcogenides such as $2H$-TaSe$_2$, $1T$-TaS$_2$, $1T$-TiSe$_2$, $1T$-TaSe$_2$, or $2H$-NbSe$_2$.[1,2] Recently, detailed aspects of the CDW in $2H$-NbSe$_2$ were investigated by comparing images taken at different bias voltages,[3] showing a spatial separation between occupied and unoccupied electronic states responsible for the CDW. This result has stimulated detailed studies of the phase of the CDW,[4] whereas STM studies are usually restricted to the amplitude of corrugation. A bias contrast dependency has also been observed on the surface CDW in Pb/Ge(111) system.[5]

STM investigations of the CDW in layered compounds have been carried out mainly on nonoxides systems. Indeed, surfaces of low-dimensional oxides are highly reactive, requiring careful preparation in a controlled atmosphere. Concerning the molybdenum oxides, a few studies have been reported on the blue bronzes cleaved in air, nitrogen, or hexadecane.[6,7] No CDW images could be obtained, suggesting the absence of CDW at the sample surface, possibly induced by the surface preparation.

We present here STM images of UHV cleaved purple potassium molybdenum bronze $K_{0.9}Mo_6O_{17}$. We have used a homemade variable-temperature microscope that will be briefly described in the following. At 40 K, well below T_p

(120 K), the CDW superstructure is clearly observed for the first time at the surface of oxides. We have also performed local tunneling spectroscopy at 40 K. We have found a depression in the LDOS around the Fermi level, which we attribute to the electronic states involved in the Peierls transition. Furthermore, by imaging simultaneously the occupied and empty states of the surface, we find a quasiperfect inversion of contrast for the CDW modulation. This is expected in compounds like $K_{0.9}Mo_6O_{17}$, which present two-dimensional (2D) Fermi surface based on three quasi-1D surfaces.

THE PURPLE BRONZES

Many characteristics of the potassium purple bronze have been studied in the last 20 years. The crystal structure is trigonal, and the lattice parameters are $a = 5.538$ Å and $c = 13.656$ Å.[8] This compound forms a layered structure with molybdenum-oxygen sheets made up of both MoO$_6$ octahedra and MoO$_4$ tetrahedra, separated by K planes. The $4d$ electrons from the molybdenum are then confined in poorly coupled infinite layers, leading to interesting quasi-2D electronic properties. Bulk $K_{0.9}Mo_6O_{17}$ undergoes at $T_p = 120$ K a CDW phase transition, but the system remains metallic below T_p.[9] Low temperature diffuse x-ray scattering and electron diffraction studies[10] have revealed satellites spots appearing at $\vec{a}*/2, \vec{b}*/2, (\vec{a}* - \vec{b}*)/2$ (we choose $\vec{a}*, \vec{b}*$, as the two in-plane reciprocal vectors). This corresponds to a Peierls lattice distortion in the real space of $(2a, 2b, c)$. Transport and thermal measurements confirmed the modification of the electronic properties in the CDW state, showing that about 50% of the carrier remained in the low-temperature phase.[9] Finally, theoretical calculations and the "hidden Fermi surface nesting concept" developed by Whangbo and co-workers[11,12] lead to a very complete understanding of the CDW transition in this compound, which is very helpful for the interpretation of STM images.

EXPERIMENT

We have recently achieved a very convenient UHV variable temperature STM that offers the possibility of cooling the sample down to 40 K, combined with a very simple handling of the sample. The STM is a beetle-type STM (Ref. 13) turned upside-down, which can be laid on top of the typical triple helix of the sample holder, using an UHV translator. The sample holder is pressed against a copper block used as a thermal reservoir, by means of tungsten springs that may simply be elongated using a linear motion feedthrough when changing the sample. The copper block is thermally insulated from the UHV chamber using a drilled stainless steel tube as suggested by Bott, Michely, and Comsa in Ref. 14. The whole block is cooled down by means of a 10-cm copper braid connected to a liquid He UHV cryostat. During low-temperature experiments, the STM itself remains almost at room temperature, so that we have only little change of the piezocoefficients of the scanner tubes. This thermal isolation is guaranteed by glass balls glued on top of the three external tubes.

Single crystals were grown by the electrolytic reduction of a melted mixture of K_2MoO_4 and MoO_3, resulting in platelets of typical size $3 \times 3 \times 0.2$ mmm^3.[8] The crystals are mounted on the sample holder, and a post is glued on the surface. The sample is cleaved by using a stainless-steel grip to pull off the post. Typical base pressure of the chamber is $5 \cdot 10^{-10}$ mb decreasing to 1.10^{-10} mb by cryosorption when cooling down. STM experiments were performed about 1 h after cooling. We used mechanically etched PtIr tips. We give here results obtained at 40 K and at room temperature, although our system allows measurements at any intermediate temperature.

RESULTS AND DISCUSSION

We present first two 8×8 nm^2 STM images of the cleaved (001) $K_{0.9}Mo_6O_{17}$ surface taken at room temperature [Fig. 1(a)] and at 40 K [Fig. 1(b)]. The inset in the upper-right part of the images is the corresponding 2D fast Fourier transform. The first image shows a hexagonal atomic pattern with spacing $a_0 = 5.5 \pm 0.1$ Å, in good agreement with the lattice parameter found in literature (5.538 Å). Notice that we rarely find surface steps in the images, and we could verify that we are dealing with atomic terraces of a few hundred nm width.

The questions that arise analyzing Fig. 1(a) are which kind of atomic plane is left at the sample surface after cleavage, and what do the white spots of the image represent? Our STM images are acquired at low bias voltage (less than 0.5 V) and then we are probing electronic states near the Fermi level. Tight-binding calculations[11] indicate that the bands crossing the Fermi level mainly come from the $4d$ orbitals of molybdenum located in the inner two Mo-O sublayers of the Mo_6O_{17} unit layer. Hence, we think that each white point of the STM image should correspond to an Mo atom of such an Mo-O plane. One can suspect that this Mo-O plane is not the actual surface plane after cleavage, but that tunneling occurs through one, two, or more insulating planes participating to the barrier. However, the low biases used in our experiments would lead in such a case to tip crashes on the surface, which very rarely happened.
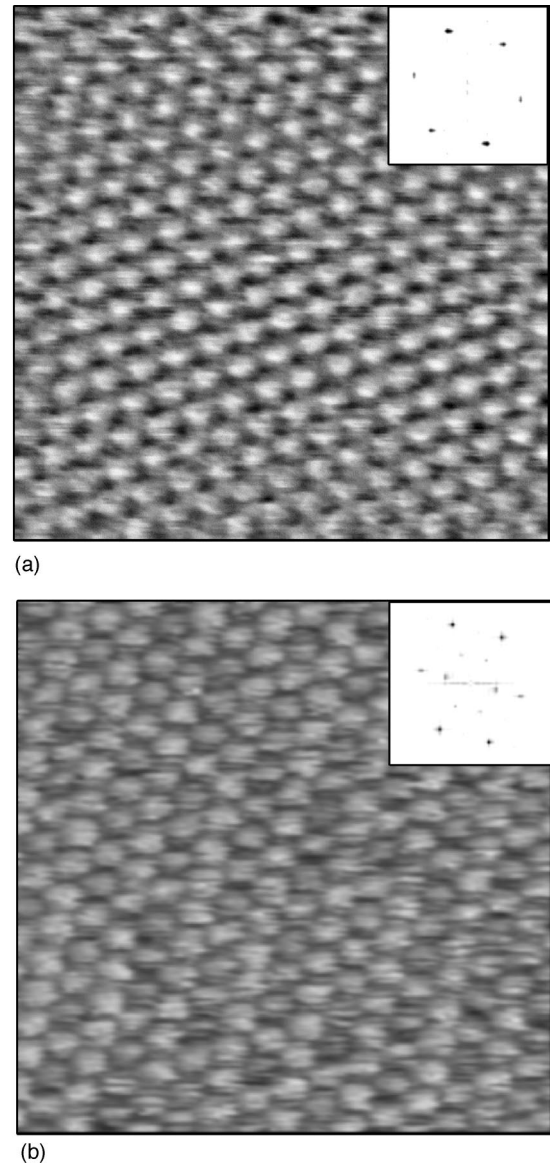

(a)

(b)

FIG. 1. 8×8 nm^2 STM images of UHV cleaved $K_{0.9}Mo_6O_{17}$. $V_{sample} = -450$ mV. On the upper-right hand we have plotted the corresponding 2D fast Fourier transform. (a) Normal phase ($T = 300$ K). The hexagonal atomic lattice is clearly resolved, with a measured parameter $a \approx 5.4 \pm 0.1$ Å. $I_{tunnel} = 150$ pA, z corrugation is 1.2 ± 0.3 Å. (b) CDW phase ($T = 40$ K). The quasi-2×2 CDW modulation is superimposed on the atomic pattern. The FFT shows the corresponding six new peaks at half the distance of the atomic lattice outer peaks. $I_{tunnel} = 400$ pA, z corrugation is 1.4 ± 0.3 Å.

Comparing images between 300 K and low temperature, a striking feature appears in the 40 K image: a very clear 2×2 hexagonal superstructure appears superimposed on the atomic pattern [Fig. 1(b)]. This result is in perfect agreement with the quasicommensurate CDW state in $K_{0.9}Mo_6O_{17}$ in which the lattice distortion leads to a unit cell that is twice the normal phase unit cell. To our knowledge, this is the first time that direct CDW visualization in oxide layered compounds is achieved, despite the numerous attempts described previously. In our opinion, the main reason for this is that in our case the cleavage has been performed in ultra-high-vacuum conditions. Another way to confirm the presence of the CDW modulation on the STM image is to make a fast
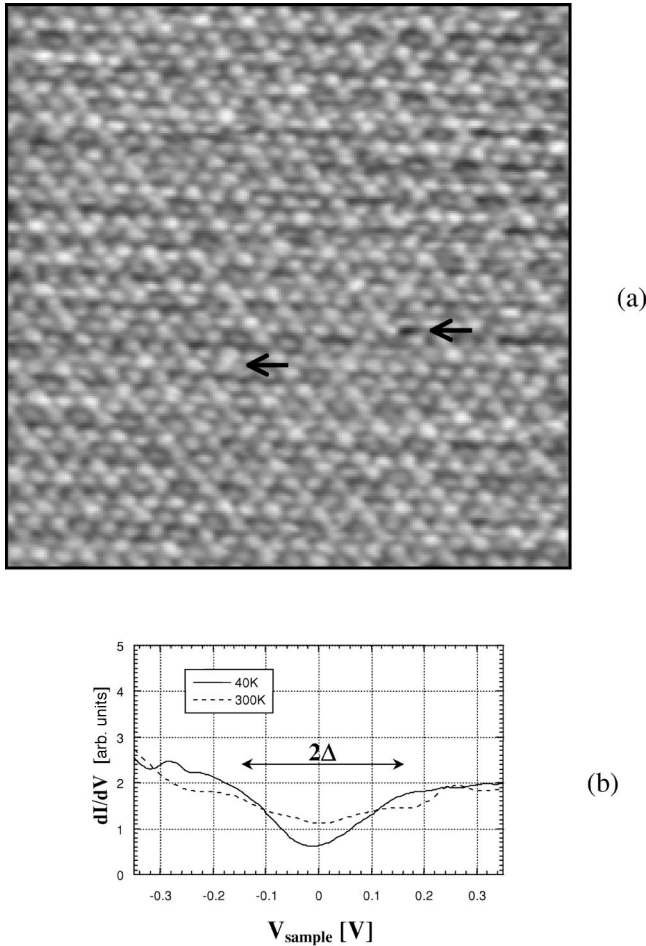
(a)

(b)

FIG. 2. (a) 13×13 nm^2 image of the CDW at 40 K. Atomic surface defects are present (indicated by arrows) but have no effect on the CDW arrangement. $V_{sample} = -400$ mV, $I_{tunnel} = 400$ pA, z corrugation is 1.4 ± 0.3 Å. (b) Scanning tunneling spectroscopy measurements recorded at 40 K (solid line) and 300 K (dashed line). The curves are an average of 64 numerical derivatives of $I(V)$ spectra obtained by opening the feedback loop for 0.5 s, for sample bias varying from -350 to $+350$ mV. Although the structures are very smooth, we measure at low temperature an important decrease of the tunneling conductance near E_F within $2\Delta = 300 \pm 50$ mV, attributed to the partial Fermi surface destruction below the Peierls transition.

Fourier transform (FFT) of the images. At low temperature [right upper hand of Fig. 1(b)], two series of peaks are present in the reciprocal space: six outer peaks due to the atomic lattice, also present in the room temperature FFT [Fig. 1(a)], and six inner peaks corresponding to the CDW $2a_0$ superstructure. This clearly demonstrates that in these quasi-2D oxides, the CDW exists up to the surface plane.
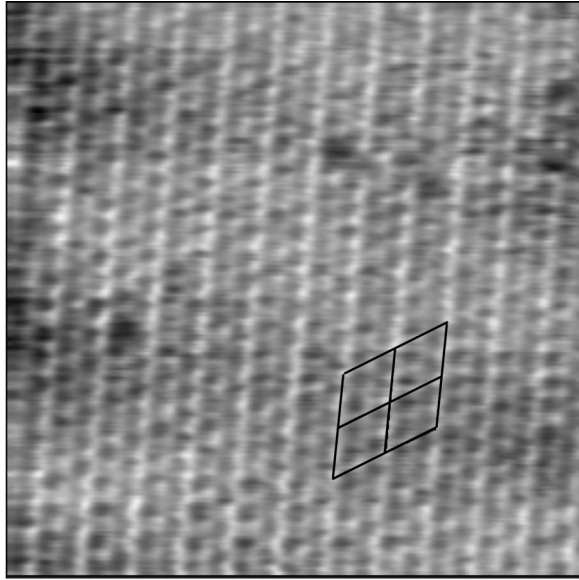
Figure 2(a) is a larger scale CDW image (13 nm), showing that the presence of few atomic defaults (indicated by arrows) does not change the CDW arrangement. We have recorded numerous images of more than 20-nm lateral size in different regions where the CDW corrugation is resolved, so that we can conclude that the CDW state is present on most of the surface plane. Very flat surfaces such as the one we got are ideal for good quality and spatially resolved tunneling spectroscopy. Usually, such measurements are made with the whole junction (tip-vacuum-sample) at low temperature

and then the tunneling conductance $dI/dV(V)$ gives a direct measurement of the LDOS at energy $eV + E_F$ (I is the tunneling current, V is the sample bias, e is the electron charge, and E_F the Fermi level). Although in the design of our STM both electrodes are not at low temperature, which increases the thermal broadening, we have acquired many spectra showing an important dip in the conductance around the Fermi level. This is shown in Fig. 2(b) where we have plotted the average of 64 curves obtained at 40 K (solid line curve), and at 300 K (dashed line). The main feature is the decrease at low temperature of the tunneling conductance near E_F, in an energy range of $2\Delta = 300 \pm 50$ meV. This value does not vary with the tip-sample distance, suggesting that we are not dealing with capacitive artifacts like Coulomb blockade. Note that we have a large uncertainty on Δ due to thermal broadening of the tip, of the order of 100 meV.
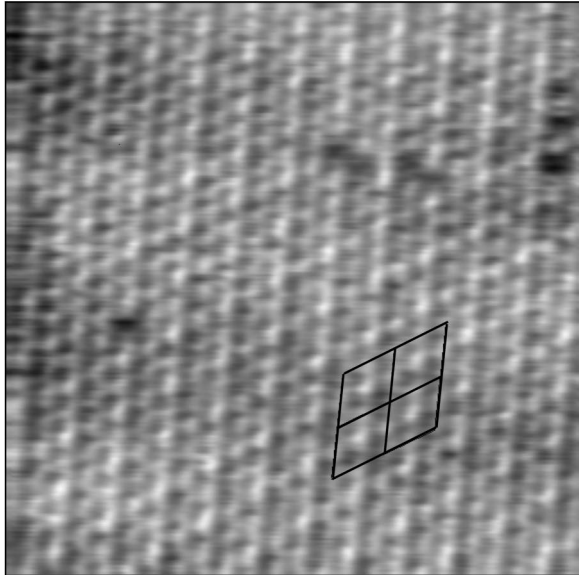
We ascribe the decrease of conductance around zero bias to the diminution of the LDOS at E_F associated with the CDW state. In the case of the purple bronze, it is known that the resistivity curve shows an important bump below T_p, suggesting that a large part of the Fermi surface is destroyed in the CDW phase.[9] It has indeed been shown that the DOS at the Fermi level is reduced by a factor of 2 or 3 in the CDW state.[15] Our spectra are in good agreement with these findings, since the conductance at E_F is lowered by almost a factor of 2 at low temperature, which is sizable for a metal/metal CDW transition. This is nicely explained by the calculations of Whangbo *et al.*,[12] where it is shown that the normal phase Fermi surface can be separated in three underlying quasi-one-dimensional surfaces, leading to ''good'' nesting properties with respect to a usual 2D material. This point has been recently highlighted with the mapping of the Fermi surface by angle-resolved photoemission spectroscopy by Gweon *et al.*[16] As a consequence, a large fraction of the Fermi surface should disappear below T_p.

Another useful feature of the STM is the possibility to image simultaneously the surface with negative and positive sample voltage, in order to get, respectively, the occupied and empty states spatial distribution. We have performed such measurements at low temperature, that means in the CDW phase. In Figs. 3(a) and 3(b), two 8×8 nm^2 topographic images are shown, simultaneously obtained at bias voltage -200 and $+200$ mV, respectively. In both images, the atomic pattern and the 2×2 CDW superstructure are present. However, it is obvious that the spatial phase of the CDW changes between the two polarities. At the same time, the atomic site position remains at the same place on both images. For a clearer analysis, we have selected four CDW unit cells on Fig. 3(a) and replotted them exactly at the same position on Fig. 3(b). The most striking result is that the minima of the CDW modulation in the center of each cell of Fig. 3(a) becomes a maxima in Fig. 3(b). This can be considered like *a quasiperfect contrast inversion of the CDW modulation*.

This result is consistent with what we could expect for a 2D system presenting a Fermi surface composed of three underlying quasi-1D surfaces. In the case of a true 1D CDW state, it has been shown[17–19] that one should find a perfect contrast reversal in STM images taken at opposite voltage around the CDW band gap. As quoted above, the peculiar
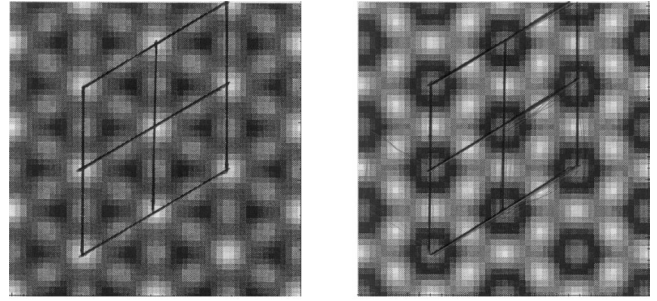
(a)

(b)

(a)   (b)

FIG. 4. Calculated images of CDW bias voltage dependency, in the simple model of three 1D CDW's at the surface (see text for explanation). (a) Filled states; (b) empty states.

take into account both the hexagonal symmetry of the surface plane and the 2×2 CDW superstructure. The calculated image is then a function $I(\vec{x})$ with $\vec{x}=(x,y)$:

$$I=I_{atoms}+I_{CDW}$$
$$=\{\cos[\vec{a}^*\vec{x}]+\cos[\vec{b}^*\vec{x}]+\cos[(\vec{a}^*-\vec{b}^*)\vec{x}]\}$$
$$+\varepsilon\{\cos[\vec{a}^*\vec{x}/2]+\cos[\vec{b}^*\vec{x}/2]+\cos[(\vec{a}^*-\vec{b}^*)\vec{x}/2]\}.$$

Occupied and empty states images correspond, respectively, to $\varepsilon=+1$ and $\varepsilon=-1$. They are shown in Figs. 4(a) and 4(b), respectively. Note that these images are not intended to reproduce the details of the topographic data, for which a sophisticated model would be required. However, they nicely illustrate the effect of contrast reversal in our STM images. Hence, we believe that the hidden 1D nesting concept introduced by Whangbo *et al.* allows a simple explanation of the present STM experiments.

CONCLUSION

This work presents STM images of CDW in metallic oxides compounds. Because of the optimal cleavage conditions and the quality of the single crystals, we were able to study at 40 K the bias dependency of the 2×2 CDW modulation. We show that occupied and empty electronic states responsible for the CDW are in opposite phase, leading to a contrast reversal of the CDW on the STM images. This is what we would expect with 1D charge density waves at the surface of a 2D compound. We believe that our experiments are totally consistent with the model of hidden 1D nesting of Whangbo *et al.*

FIG. 3. Two 12×12 nm^2 topographic images taken at 40 K in the $+/-$ V_{sample} simultaneous mode ($I_{tunnel}=500$ pA, z corrugation is 1.4 ± 0.3 Å). (a) $V_{sample}=-200$ mV; (b) $V_{sample}=+200$ mV. Four CDW unit cells drawn at the same position on the images show an almost perfect contrast reversal of the CDW pattern, although the atomic sites remain unchanged.

topology of the Fermi surface of the purple bronze suggests that the low-temperature phase can consist (in a first approximation) of a superposition of three 1D/CDW's. This should give rise to contrast reversal at opposite polarities, in agreement with our observations. Note that contrast reversal is not a general property of CDW's in 2D materials, since it is not observed in $2H$-NbSe$_2$.[3,4]

In order to verify that our images could be reproduced in this 1D framework, we have adopted a simple model in which the atomic lattice is represented by a sum of three cosine functions with periodicity $\vec{a}^*,\vec{b}^*$ and $(\vec{a}^*-\vec{b}^*)$, and the CDW state by a sum of three cosine functions with periodicity $\vec{a}^*/2$, $\vec{b}^*/2$ and $(\vec{a}^*-\vec{b}^*)/2$. In this approach, we

[1] R. V. Coleman, B. Drake, P. K. Hansma, and G. Slough, Phys. Rev. Lett. **55**, 394 (1985).

[2] R. V. Coleman, Zhenxi Dai, W. W. McNairy, C. G. Slough, and Chen Wang, in *Scanning Tunneling Microscopy*, edited by J. A. Stroscio and W. J. Kaiser (Academic, San Diego, 1993).

[3] P. Mallet, W. Sacks, D. Roditchev, D. Défourneau, and J. Klein, J. Vac. Sci. Technol. B **14**, 1070 (1996).

[4] W. Sacks, D. Roditchev, and J. Klein, Phys. Rev. B **57**, 13 118 (1998).

[5] J. M. Carpinelli, H. H. Weitering, E. W. Plummer, and R. Stumpf, Nature (London) **381**, 398 (1996).

[6] U. Walter, R. E. Thomson, B. Burk, M. F. Crommie, A. Zettl, and John Clarke, Phys. Rev. B **45**, 11 474 (1992).

[7] S. Tanaka, E. Ueda, and M. Sato, Solid State Commun. **87**, 877 (1993).

[8] H. Vincent, M. Ghedira, J. Marcus, J. Mercier, and C. Schlenker, L. Solid State Chem. **47**, 113 (1983).

[9] R. Buder, J. Devenyi, J. Dumas, J. Marcus, J. Mercier, and C. Schlenker, J. Phys. (France) **43**, L59 (1982).

[10] C. Escribe-Filippini, K. Konaté, J. Marcus, C. Schlenker, R. Almairac, R. Ayroles, and C. Roucau, Philos. Mag. B **50**, 321 (1984).

[11] M.-H. Whangbo, E. Canadell, and C. Schlenker, J. Am. Chem. Soc. **109**, 6309 (1987).

[12] M.-H. Whangbo, E. Canadell, P. Foury, and J.-P. Pouget, Science **252**, 96 (1991).

[13] K. Besocke, Surf. Sci. **181**, 145 (1987).

[14] Michael Bott, Thomas Michely, and George Comsa, Rev. Sci. Instrum. **66**, 4135 (1995).

[15] C. Schlenker *et al.*, in *Low-Dimensional Electronic Properties of Molybdenum Bronzes and Oxides*, edited by C. Schlenker (Kluwer, Dordrecht, 1989).

[16] G.-H. Gweon, J. A. Clack, Y. X. Zhang, J. W. Allen, D. M. Poirier, P. J. Benning, C. G. Olson, J. Marcus, and C. Schlenker, Phys. Rev. B **55**, 13 353 (1997).

[17] M. H. Whangbo, J. Chem. Phys. **73**, 3854 (1980).

[18] J. Tersoff, Phys. Rev. Lett. **57**, 440 (1986).

[19] G. Grüner and A. Zettl, Phys. Rep. **119**, 117 (1985).